# Design and Performance Simulation of Direct Drive Hub Motor Based on Improved Genetic Algorithm

Zhong-Shu Liu[1,2](✉)

[1] School of Information Science and Engineering, Fujian University of Technology, Fuzhou 350118, China
lzs@fjut.edu.cn
[2] The Key Laboratory for Automotive Electronics and Electric Drive of Fujian Province, Fujian University of Technology, Fuzhou 350118, China

**Abstract.** By using improved genetic algorithm (IGA), a direct drive hub motor with high efficiency and low-cost was designed. According to the characteristics of the hub motor, a mathematical model for optimize of direct drive hub motor was established, and optimized calculation was extended, and finally a prototype was developed. The simulation results show that the novel direct-drive hub motor can meet the requirements of great torque when low speed and high speed when constant power, so it is very suitable for the vehicle.

**Keywords:** Improve · Genetic algorithm · Direct drive · Hub motor · Simulation

## 1 Introduction

Due to the shortage of energy and environmental pollution, the development of electric vehicle has become the focus of national governments. The motor drive system is the core component of electric vehicle, and its driving mode can be grouped into two categories: centralized motor drive and hub motor drive. Motor drive is a new way of electric vehicle drive, it changes the power transmission hardware connection into wheel connection, saves the mechanical manipulation of shifting device which the traditional cars required, all of above makes the car drive structure be greatly simplified, each of the electrical control system of electric wheel can be easy to implement and braking energy feedback be easy to achieve. There are two driving modes of hub motor, namely, direct drive and wheel side reducer. In this paper, the direct drive outer rotor hub motor is studied, and its structure is shown in Fig. 1, it is an outer rotor three-phase permanent magnet synchronous motor (PMSM) with great torque when low speed and high speed when constant power, meanwhile, it does not need retarding mechanism, which makes the drive system be simple and efficiency be further improved [1].

The hub motor designed in this paper has advantages of high power density, high efficiency, simple structure, great starting torque and strong ability for overload. Optimum design of hub motor is a process to change engineer problem into optimal


P. Krömer et al. (eds.), *Proceedings of the Fourth Euro-China Conference on Intelligent Data Analysis and Applications*, Advances in Intelligent Systems and Computing 682, DOI 10.1007/978-3-319-68527-4_33

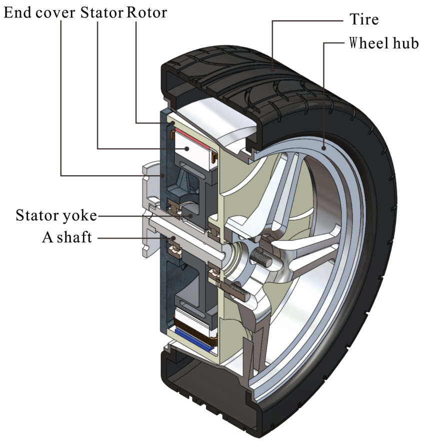


**Fig. 1.** Structure of direct drive motor

problem, it is a complex problem of nonlinear, constrained, discrete and the traditional optimization algorithm is difficult to find the global optimal solution of the hub motor. In this paper, based on the study of permanent magnet synchronous motor, according to the characteristics of the direct drive hub motor [2], an three-phase permanent magnet synchronous motor (PMSM) used as direct drive motor was developed by using improved genetic algorithm (IGA).

# 2 Improved Genetic Algorithm

## 2.1 Improved Genetic Algorithm

The basic idea of improved genetic algorithm is using adaptive crossover operator and mutation operator of genetic algorithm to optimize the initial scheme, thus the optimized solutions can be used as the initial scheme of pattern search method, finally, a global optimal solution with highest efficiency is obtained.

Due to the accuracy and efficiency of crossover rate and mutation rate of genetic algorithm depending on the fitness of population individual, when the fitness is bigger, in order to ensure that reduce the probability of genetic damage, an individual will use the smaller crossover rate and mutation rate [3], while fitness is small, in order to ensure its searching area, the individual will use the bigger crossover rate and mutation rate, therefore, the crossover operator $p_c$ and mutation operator $p_v$ of improved genetic algorithm (IGA) are shown as follows

$$p_c = \begin{cases} p_{c1}, f' > f'_{avg} \\ \frac{p_{c1} - p_{c2}}{2}, \cos\left[\frac{f - f_{avg}}{f_{\min} - f_{avg}} \pi\right] + \frac{p_{c1} + p_{c2}}{2}, f' \le f'_{avg} \end{cases} \tag{1}$$

$$p_v = \begin{cases} p_{v1}, f' > f'_{avg} \\ \frac{p_{v1} - p_{v2}}{2}, \cos\left[\frac{f - f_{avg}}{f_{\min} - f_{avg}}\pi\right] + \frac{p_{v1} + p_{v2}}{2}, f' \le f'_{avg} \end{cases} \tag{2}$$

In formula (1) and (2), $p_{c1}$ and $p_{v1} \in (0, 1)$, $f_{\min}$ is the minimum fitness of the group; $f_{avg}$ is the average fitness for each generation group; $f'$ is the smaller fitness of the two individuals crossing; $f'_{avg}$ is the average fitness of the variation individuals. After improving the crossover and mutation rates of improved genetic algorithm (IGA), the calculation flow chart is shown in Fig. 2.

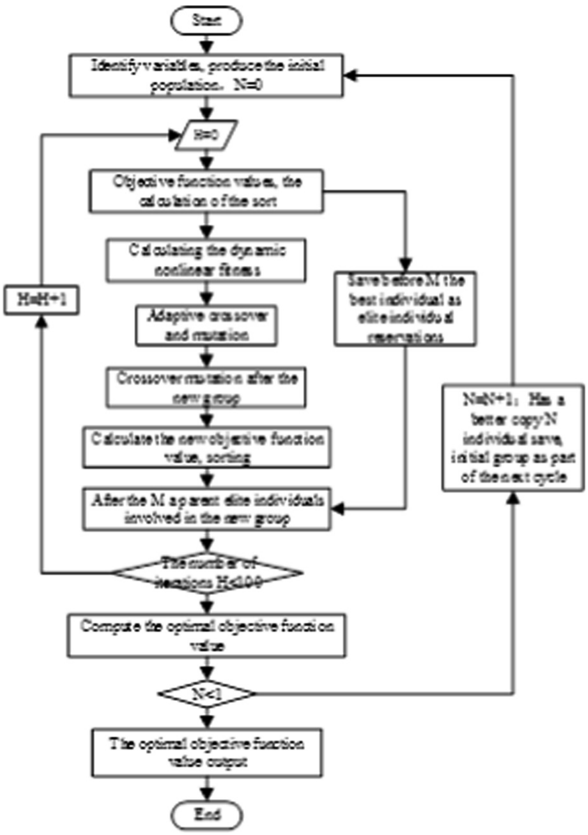

**Fig. 2.** IGA algorithm flow chart of PMSM

## 2.2 Overall Electromagnetic Structure Design

To select objective function and optimization variable is very important in optimization design of direct drive hub motor. To comprehensively consider the performance and cost of hub motor, the difficulty of processing, the structure arrangement and other factors, the objective function of the hub motor is defined as the cost of a three-phase permanent magnet synchronous motor corresponding to per unit efficiency. That is:

$$f(x) = \min \frac{F(x)}{\eta} = \min \frac{(m_{cu}t_{cu} + m_{Fe}t_{Fe} + m_m t_m)}{P_1 - \sum p} P_1 \tag{3}$$

In above, $m_{cu}$ is the price for the copper materials; $m_{Fe}$ is the price of steel materials; $m_m$ is the price of nd-fe-b materials; $t_{cu}$ is the total weight of copper materials used; $t_{Fe}$ is the total weight of the steel materials used for; $t_m$ is the total weight of nd-fe-b permanent magnet materials. $P_1$ is the input power of the motor; $\sum p$ is the total loss of the motor [4].

The following parameters of the permanent magnet synchronous motor are selected as the optimal design variables:

Rotor outer diameter $D_2$; rotor inner diameter $D_{i2}$; stator outer diameter $D_1$; stator inner diameter $D_{i1}$; length of core $l_{eff}$; permanent magnet thickness $h_m$ and the width of the permanent magnet $b_m$, namely:

$$X = \begin{bmatrix} x_1 & x_2 & x_3 & x_4 & x_5 & x_6 & x_7 \end{bmatrix}^T = \begin{bmatrix} D_2 & D_{i2} & D_1 & D_{i1} & l_{eff} & h_m & b_m \end{bmatrix}^T \tag{4}$$

The constraints of optimization design of hub motor include boundary constraint and performance constraint, the constraint conditions in this paper according to the engineering simulation and the performance requirement in design of three-phase permanent magnet synchronous motor are as follows: the starting current $I_{\text{st}}$. the starting torque $T_{\text{st}}$; rated speed $n_{\text{N}}$; heat load $H$ and air gap magnetic induction intensity $B_\delta$. That is:

$$\begin{aligned} & g(1) = \frac{I_{st} - I_{st0}}{I_{st0}} \le 0; g(2) = \frac{T_{st} - T_{st0}}{T_{st0}} \le 0; g(3) = \frac{n_N - n_{N0}}{n_{N0}} \le 0; \\ & g(4) = \frac{H - H_0}{H_0} \le 0; g(5) = \frac{B_\delta - B_{\delta 0}}{B_{\delta 0}} \le 0 \end{aligned} \tag{5}$$

## 2.3 Stator Winding Design

Stator winding design is an important part of hub motor design, which can be divided into two types: centralized winding and distributed winding. The objective of design for stator winding is to make gap magnetic field distribution close to sine wave. The main difference between the centralized and distributed windings of the stator is the winding pitch, centralized winding pitch is 1, which means two effective edges of each coil of the motor across a tooth [5], and distributed winding pitch is greater than 1, which means the two effective edges of each coil across the slot number greater than 1. The end part of the centralized winding is small and the winding process is simple, which makes the hub motor have a better electromagnetic performance and a lower copper loss and higher efficiency [6]. The hub motor stator winding designed in this paper have a centralized winding, which is shown in Fig. 3.

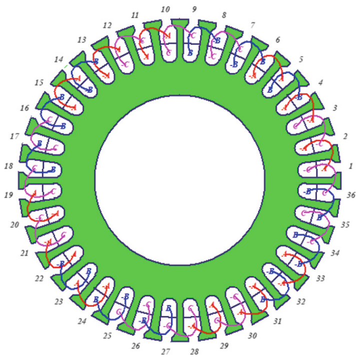

**Fig. 3.** Centralized winding wiring diagram

### 2.4 Measures to Reduce the Cogging Torque

The cogging torque of the motor is an endemism in permanent magnetic synchronous motor (PMSM), it is a reluctance torque caused by the interaction between the stator core slot and permanent magnet in rotor, which will cause vibration and noise in the motor, and affect the speed control system of low speed performance and positioning accuracy of position control system. At present, there are various measures to reduce the cogging torque of permanent magnet motor, such as magnetic pole deviation, magnetic pole eccentric, and slot [7].

In this paper, the cogging torque is reduced by two measures as following:

#### 2.4.1 Inner Stator Chute

This method is to adjust the phase relationship of the unit tooth groove torque at the superposition, which can make each other cancel out. In theory, the stator groove tilting a stator pitch relative to the rotor could eliminate the cogging torque completely. After taking all the factors into consideration, we adopted the chute stator iron with 1.5 times pitch in the prototype.

#### 2.4.2 Optimizing z/2p

In above, z means the stator slot number and 2p means the poles of rotor. By using least common multiple (LCM) of the slot number and the poles of rotor to calculate the minimum order number of cogging torque. It is known that the greater the number of the cycle of fundamental wave of the cogging torque [8], the smaller the amplitude. So we should choose the least common multiple (LCM) as larger as possible, and through the magnitude of least common multiple (LCM) to calculate minimum order of cogging torque [8].

The analysis result shows that in order to reduce the cogging torque, we should choose the LCM as large as possible In view of the manufacturing process and cost factors, the z/2p ratio of the motor in this paper is chosen to be 36/20 and it equals 180. So the minimum order of cogging torque equals $K = LCM/Z = 180/36 = 5$, which means all cogging torque less than 5 order will be eliminated. The cogging torque curve is shown in Fig. 4.

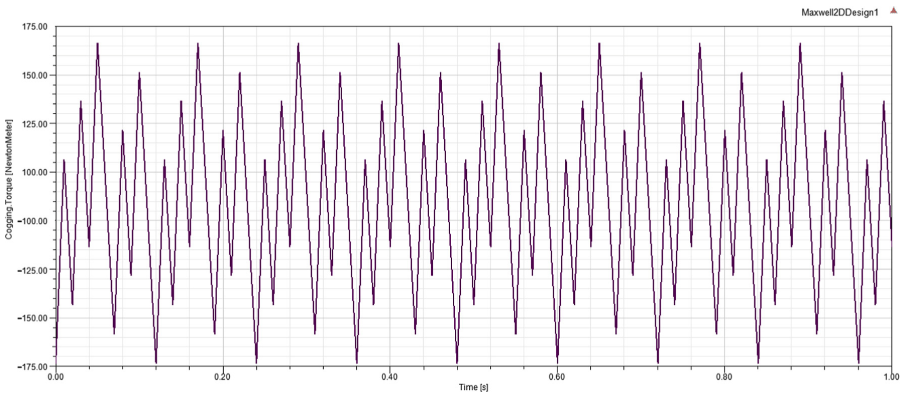


**Fig. 4.** Cogging torque of hub motor

### 2.5 Optimum Design Result

Based on theory above and method of the improved genetic algorithm, optimize the hub motor electromagnetic structure, the result is as follows: rated voltage 255 v, rated power 45 kw, poles of rotor 20, stator slots 36, double-layer centralized stator winding, Y connection. The structural parameters are shown in Table 1.

**Table 1.** Structural parameters of hub motor

| Parameter | Value | Parameter | Value |
|---|---|---|---|
| Outer diameter of the stator | 270/mm | Outer diameter of the rotor | 303/mm |
| Inner diameter of the stator | 190/mm | Inner diameter of the rotor | 283/mm |
| The length of the core | 55/mm | The air gap length | 1.5/mm |
| The thickness of the magnet | 5/mm | Slot number | 36 |
| The width of the magnet | 30/mm | Pole | 20 |

## 3 Finite Element Analysis of Magnetic Field

### 3.1 Grid Subdivision

Now we will analyze the hub motor by using two-dimensional finite element method, which is a numerical calculation method based on discretization. Figure 5 is the grid subdivision of hub motor designed in this paper. It can be seen from Fig. 5 that the grid density of stator and rotor would be minimum while the grid density of air gap would be maximum. So using different grid density subdivision we can save computing resources and ensure the accuracy of the calculation [9].

### 3.2 Analysis of the Hub Motor Internal Electromagnetic Field

Using Ansoft Maxwell we can analyze the flux density distribution of cloud of generator shown in Fig. 6(a) when it is in no-load. It can be seen from the diagram, the flux

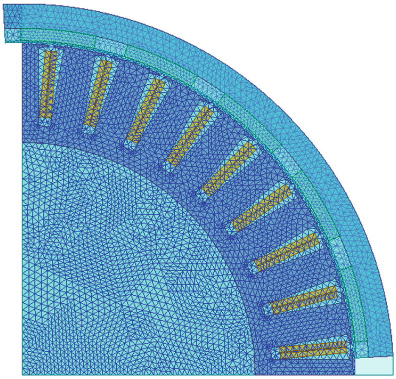

**Fig. 5.** Grid division of hub motor

density value of stator yoke of motor is maximum which has reached 2.71 T, we can get the flux density distribution of cloud of generator shown in Fig. 6(b) when it is in load. Compared with Fig. 6(a), we found that when the motor is in load, the iron core saturation degree decrease relative to the case in no-load, motor stator yoke of flux density value decrease to 2.58 T, at the same time, all parts of the stator iron core flux density amplitude is decreasing, the center line of the air-gap magnetic field of electric skewed compared with no-load, the reason is that the armature reaction weakens the air gap field and causes gap magnetic field distortion.

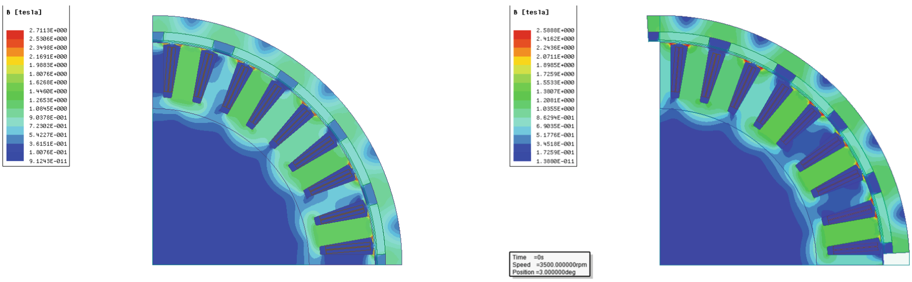

a) No-load b) In-load

**Fig. 6.** Flux density cloud diagram of hub motor

We could make a conclusion from above that the magnetic flux near the stator and rotor yoke and the air gap are saturated relatively, and the field distribution of motor is reasonable. It does not exist local magnetic oversaturation and the prototype meets the design requirements [10].

## 4 Performance Calculation and Simulation

Using Simplorer software we build main circuit and control circuit model of hub motor as following, when setting up main circuit model we can select related components in the model library [11], and then use wire connects them according to the actual structure of the circuit. The control circuit model is established by using state machine. Figure 7 is the simulation model of hub motor system.

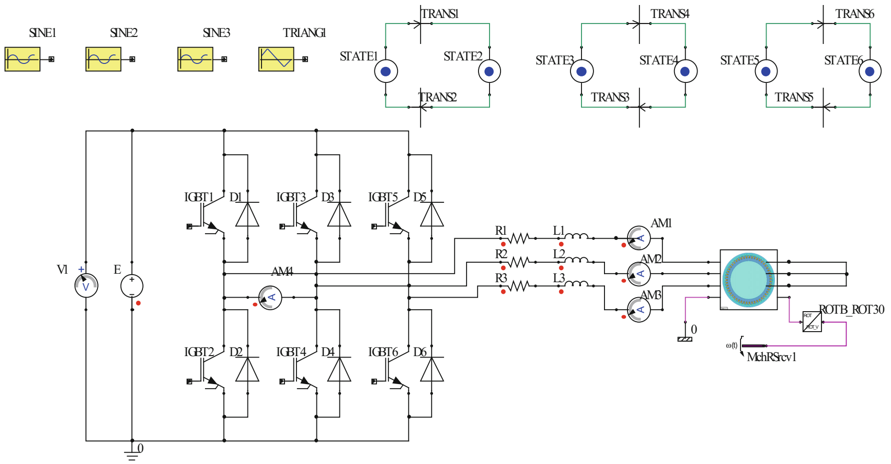


**Fig. 7.** Hub motor system circuit model diagram

### 4.1 Electric Motive Force (EMF)

Using Maxwell simulation software, the EMF waveform of the motor running at 3500 rpm is shown in Fig. 8. It can be seen from the figure that the sinusoidal of the EMF waveform is perfect [12], which indicating that the improved genetic algorithm design has a remarkable effect. Simulation calculation shows that when the phase voltage peak is 160 V, the maximum speed of the motor is 3500 r/min, which means the result meets the design requirement [13].

### 4.2 Torque Characteristics

The torque characteristic of the hub motor is shown in the Fig. 9. From the characteristic it can be seen that the motor has great starting torque and small torque ripple, so it is very suitable for the vehicle [14].

### 4.3 Input Voltage and Input Current Characteristics

The input voltage and input current waveform of generator when it is in-load cases are shown in Fig. 10(a) and (b) respectively. As it can be seen from the diagram, they are all sine wave without distortion, the peak value of them are 375 V and 200 A

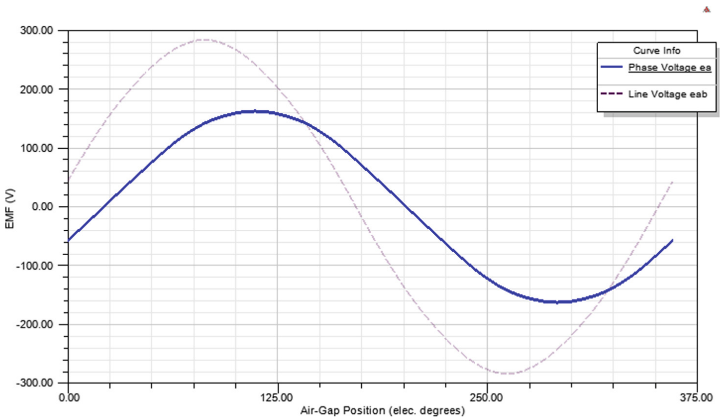


**Fig. 8.** EMF waveform diagram of hub motor

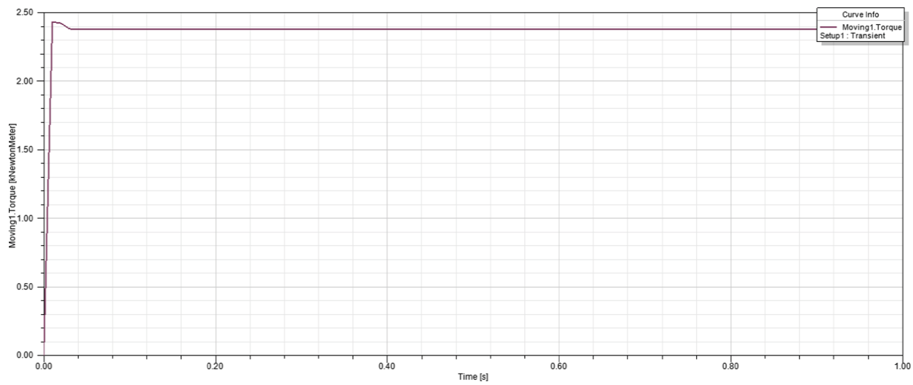


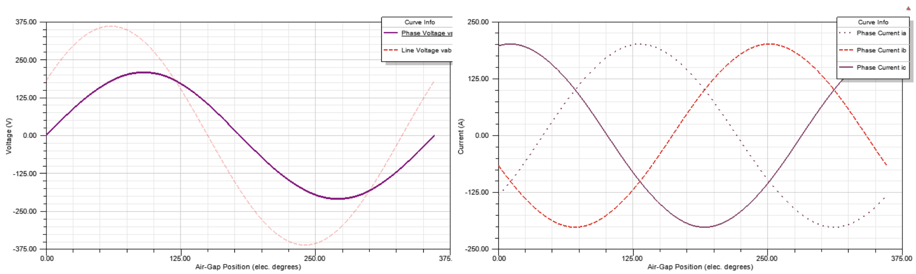


**Fig. 9.** Torque characteristics

a) Voltage b) Current

**Fig. 10.** Input voltage and input current characteristics

respectively, and the effective value of them equals 262 V and 131 V, the input power equals 46 KW, which meet the design requirement fully.

### 4.4 Efficiency Characteristics

The efficiency characteristic of hub motor is shown in the Fig. 11. It can be seen from the figure that the rated efficiency of the motor is 96% and the design target has been reached [15].

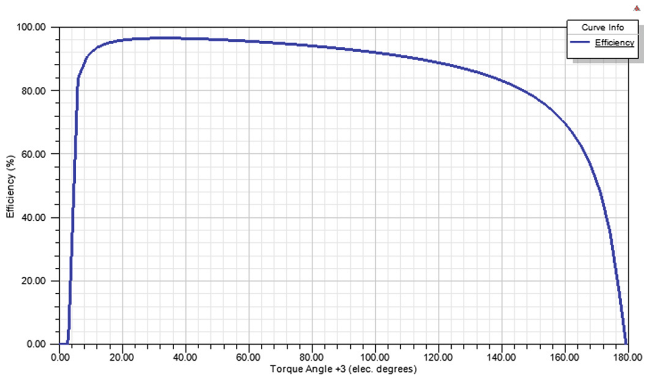


**Fig. 11.** Efficiency characteristics

## 5 Conclusion

Direct drive hub motor has become a new development trend of vehicle. In this paper, a direct drive hub motor is designed based on improved genetic algorithm (IGA). The simulation results show that the electric motor has the characteristics of great torque when low speed, fast response, low torque ripple, high efficiency and low-cost. The above results show that design of prototype is reasonable.

**Acknowledgment.** This research was supported by the Natural Science Foundation of Fujian Province of China. (Grant No. 2017J01667).

## References

1. Chen, Q., Shu, H., Ren, K., Chen, L., Chen, B., Xie, A.: Optimization design of driving in-wheel motor of micro-electric vehicle based on improvement genetic algorithm. J. Cent. S. Univ. (Sci. Technol) **43**(8), 3013–3017 (2012)
2. Lei, L., Hu, Y., Song, Z., Chen, Y., Zhang, H.: Design of outer rotor hub motor for electric vehicle. Micromotors **49**(10), 6–9 (2016)
3. Li, S., An, R., Xu, Z., Dong, W.: Coordinated LVRT of IG and PMSG in hybrid wind farm. Electr. Power Autom. **35**(2), 21–27 (2015)

4. Lu, D., Ouyang, M., Gu, J., Li, J.: Field oriented control of permanent magnet brushless hub motor in electric vehicle. Electr. Mach. Control **16**(11), 76–83 (2016)
5. Chen, G., Tang, N., Li, D.: Optimization design of PMSG based on improved genetic algorithm. Explosion-Proof Electr. Mach. **46**(1), 5–9 (2011)
6. Wang, X., Gao, P.: Analysis of 3-D temperature of in-wheel motor with inner-oil improved cooling for electric vehicle. Electr. Mach. Control **20**(3), 36–41 (2012)
7. Shen, X., Zhao, Q., Xu, P.: Control research on maximum power of the direct-drive permanent magnet synchronous rotor. J. Electr. Power **29**(1), 28–31 (2014)
8. Gao, J.: Research on design technology and application of direct-drive permanent magnet rotor with wind turbine. Ph.D, Hunan University, Changsha, pp. 36–55 (2013)
9. Kun, Y., Xiu, Y.: Modeling optimization and simulation of grid-connected direct-driven permanent magnet wind power system based on small signal stability analysis. East China Electr. Power **42**(10), 2028–2033 (2014)
10. Zhai, Y.: Research on vector control of PMSG in low temperature waste heat power generation system. Ph.D., Shenyang University of Technology, Shenyang, pp. 17–30 (2015)
11. Feng, H., Huo, Z., Hu, X.: Constant power control for wind turbine based on finite-time method. Renew. Energy Resour. **33**(12), 1831–1834 (2015)
12. Shen, J., Miao, D.: Variable Speed permanent magnet synchronous generator systems and control strategies. Trans. China Electrotech. Soc. **28**(3), 2–8 (2013)
13. An, Q., Li, S., Lizhi, S.: Research on novel open-end wind permanent magnet synchronous motor vector control systems. Proc. CSEE **35**(22), 5891–5898 (2015)
14. Sun, M.: Design and flux-weaking control for in-wheel –motor of electric vehicle, pp. 36–55 Ph.D., Harbin Institute of Tecnology, Harbin (2009)
15. Weng, M., Li, Q., Cao, M.: Parameters calculation and structure design for wheel hub permanent magnet brushless direct current motor of drive method. Electr. Mach. Control Appl. **42**(7), 12–15 (2015)